crystals

MDPI

*Article*

# Halide Ion Embraces in Tris(2,2′-bipyridine)metal Complexes

**Edwin C. Constable * and Catherine E. Housecroft**

Department of Chemistry, University of Basel, BPR 1096, Mattenstrasse 24a, CH-4058 Basel, Switzerland; catherine.housecroft@unibas.ch

* Correspondence: edwin.constable@unibas.ch; Tel.: +41-61-207-1001

Received: 27 July 2020; Accepted: 1 August 2020; Published: 3 August 2020


**Abstract:** An analysis of the $[M(bpy)_3]^{n+}$ (bpy = 2,2′-bipyridine) complexes with halide counterions in the Cambridge Structural Database reveals a common structural motif in two thirds of the compounds. This interaction involves the formation of 12 short C–H ... X contacts between halide ions lying within sheets of the cations and H-3 and H-3′ of six $[M(bpy)_3]^{n+}$ complex cations. A second motif, also involving 12 short contacts, but with H-6 and H-5, is identified between halide ions lying between sheets of the $[M(bpy)_3]^{n+}$ cations.

**Keywords:** metal complexes; 2,2′-bipyridine; halide; C–H ... X interactions

## 1. Introduction

The established crystallographic databases, including the Inorganic Crystal Structure Database [1], the NIST Inorganic Crystal Structure Database [2], the Protein Data Bank [3–5] and the Cambridge Structural Database (CSD) [6,7], have created unprecedented opportunities for data mining and investigating the intramolecular, intermolecular and supramolecular interactions, which are important in determining the spatial arrangement, orientation and packing of molecules and ions in crystal lattices. For the molecular scientist, the visualization program Mercury [8] and the search software Conquest [9], both incorporated within the CSD, are of particular utility. The opportunities presented for the probing and understanding of the intimate details of crystal packing sometimes result in losing the relationship with general chemical properties and reactivity. In many cases, "weak" interactions, such as van der Waals forces, are typically unimportant in solution behaviour. Nevertheless, the field of crystal engineering has emerged predicated upon the importance of weak interactions, including π-π and C–H-π interactions, as well as halide, pnictide and tetrel bonds in the solid state. However, when "moderate" or "strong" interactions are present in the solid-state structure of a compound, it is appropriate to consider their relevance in its more general chemistry.

A few years ago we noticed dramatic variations in the performance of (apparently) chemically similar batches of $[Ir(bpy)(ppy)_2](PF_6)$ (Hppy = 2-phenylpyridine, bpy = 2,2′-bipyridine) in light-emitting electrochemical cells [10]. This was shown to be due to the carrying through of small amounts of chloride ions from the synthesis and was demonstrated as a significant solution interaction by $^1$H NMR spectroscopic titrations of solutions of $[Ir(bpy)(ppy)_2](PF_6)$ with $[^nBu_4N]Cl$. A solid state structural determination of the compound $[Ir(bpy)(ppy)_2]Cl{\cdot}2CH_2Cl_2{\cdot}[H_3O]{\cdot}Cl$ revealed a chloride ion lying close to H-3 and H-3′ of the bpy ligand (H ... Cl, 2.674 and 2.739 Å; C ... Cl, 3.627 and 3.794 Å; ∠C–H ... Cl, 145.84 and 163.19°; Figure 1a) and we described the interaction as a bifurcated hydrogen bond (Figure 1b). The combination of a crystallographically significant solid-state interaction with related solution behaviour allowed us to interpret the phenomenon in terms of the known acidity of H-3 and H-3′ in the bpy complexes [11–19]. Although we are well aware of the dangers of using distance criteria

for assessing weak interactions [20–22], the H . . . X distances provide a convenient metric for a first triage of structural data.

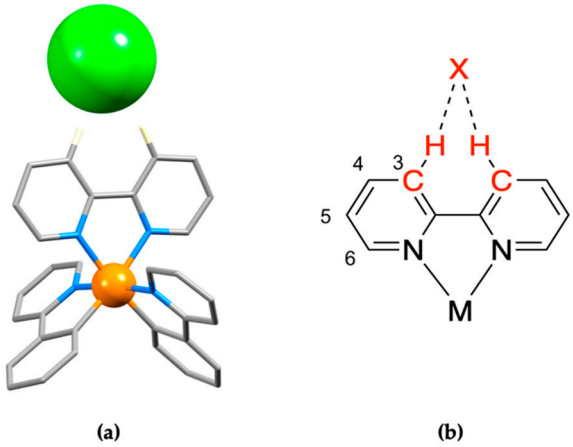


**Figure 1.** (**a**) The chloride ion interaction with H-3 and H-3′ of the 2,2′-bipyridine ligand in the complex $[Ir(bpy)(ppy)_2]Cl{\cdot}2CH_2Cl_2{\cdot}[H_3O]{\cdot}Cl$ (Hppy = 2-phenylpyridine, bpy = 2,2′-bipyridine) [10]. The chloride ion is shown in a space-filling representation; only the hydrogen atoms involved in the interaction with the chloride ion are shown. The hydrogen atom positions are normalized (C–H = 1.089 Å) and the H . . . Cl distances are 2.674 and 2.739 Å; (**b**) the generic representation of the bifurcated hydrogen bond to H-3 and H-3′ of a 2,2′-bipyridine ligand. The atoms in red are those used to define the various metrical parameters.

In this article, we show that the interaction of the halide or halogen atoms with the H-3 and H-3′ atoms of the oligopyridine ligands in metal complexes is a recurrent phenomenon in $[M(bpy)_3]^{n+}$ complexes and generates a common structural motif.

## 2. The Choice of Metal Complex Scaffold

### *2.1. The Oligopyridines*

We selected the oligopyridines as the metal-binding domains for this study. There is a large body of crystallographic data for metal complexes of these ligands in the Cambridge Structural Database (using version 5.41) and we have, in general, restricted our coverage to complexes containing the parent compound 2,2′-bipyridine in order to eliminate the influence of other interactions between the halogen and substituents on the ligand. Furthermore, the chemistry of these ligands and their complexes is exceptionally well documented [23–36], facilitating correlations between the solid-state features and chemical behaviour.

### *2.2. Supramolecular Interactions in Oligopyridine Complexes*

Oligopyridine metal-binding domains played a key role in the development of supramolecular and metallosupramolecular [37–40] chemistry. The oligopyridines provide an ideal scaffold to investigate supramolecular interactions as they interact with most of the elements in the periodic table. Dance has identified a variety of types of supramolecular embraces between the cations in "simple" oligopyridine complexes as well as a number of cation–anion interactions in these species [41–58]. In many cases, these interactions, described as "embraces" by Dance, are responsible for the assembly of the cationic lattice, which acts as the host for the anionic guests that are the focus of this article.

### *2.3. Outer-Sphere Complexes and Ion-Pairing*

Interactions at the periphery of metal complexes have been known to be of importance for many years, although they have not always been associated with the term "supramolecular". The structural

studies of Nassimbeni have been particularly important in identifying the commonest types of interactions and provide a solid body of evidence for the hydrogen-bonding interactions with Werner-type coordination compounds [59–65]. Studies such as these relate directly to the "outer-sphere" complexes implicated in studies of substitution mechanisms, in which the incoming ligands are non-covalently associated with the starting complexes (A-type mechanisms) or intermediates (D-type mechanisms) [66,67]. Of particular importance are kinetic and thermodynamic studies, establishing both the nature and strength of the outer-sphere interactions between the oligopyridine complexes and halides and their relevance to the reaction chemistry of these species [68–78].

### *2.4. Methodology*

Conquest (version 2020.1) [9] was used for the primary triage of structures in the database. For the complexes with simple halide anions, the halogen atom was constrained to have the number of bonded atoms = 0 and one of the two nitrogens of a 2,2′-bipyridine was bonded with the bond-type "Any" to any metal (atom type 4M). Hydrogen atoms were added explicitly to the 3 and 3′-positions of the 2,2′-bipyridine ligands. This allowed the identification of complexes containing coordinated oligopyridines (but not 1,10-phenanthrolines) and at least one "free" halide ion in the lattice, and the results for the four halide ions are summarized in Table 1. In all searches, normalized C–H distances of 1.089 Å were specified. A preliminary analysis of these data indicated that the presence of multiple ligand types in heteroleptic complexes made the interpretation and identification of the structural paradigms very difficult and we made the decision to consider only complexes containing at least one 2,2′-bipyridine ligand and subsequently restricted the searches to homoleptic 2,2′-bipyridine complexes for the in-depth analysis.

**Table 1.** Metal oligopyridine complexes containing halide anions found in the Cambridge Structural Database (version 5.41).

| Halide | Number of Hits | Number of Hits Containing a 2,2′-bipyridine Ligand | Number of Hits for $[M(bpy)_3]^{n+}$ Complexes |
|---|---|---|---|
| F | 7 | 5 | 0 |
| Cl | 643 | 270 | 47 |
| Br | 126 | 46 | 9 |
| I | 105 | 53 | 8 |

For the subsequent analysis of all data, normalized hydrogen positions were used for the C–H bonds (C–H = 1.089 Å). All graphical representations were generated using Mercury 2020.1 [8] and saved as POV-Ray files and subsequently rendered using POV-Ray v. 3.7.0.8 unofficial [79]. All hydrogen atoms, other than those involved in the interactions with halide or halogen, are generally omitted from the representations whilst the halogen atoms involved in the H . . . X interactions are represented in a space-filling mode.

## 3. Ubiquitous Interactions in $[M(bpy)_3]^{n+}$ Complexes

Typically, the cations in $[M(bpy)_3]^{n+}$ complexes form layer structures with extensive supramolecular interactions between the aromatic ligands [41–58]. Anions can be located between the layers of the cations or within them. These two arrangements give rise to different structural archetypes in the complexes with halide anions.

Of the 64 hits for $[M(bpy)_3]^{n+}$ complexes in the CSD (Table 1), only 55 have had their 3D coordinates deposited. Accordingly, the compounds Λ-$[Ru(bpy)_3]_2(C_4H_4O_6)Cl_2{\cdot}12H_2O$ (Refcode BUDLAN) [80], Λ-$[Fe(bpy)_3]_2(C_4H_4O_6)Br_2{\cdot}11H_2O$ (Refcode BUDLER) [80], Λ-$[Co(bpy)_3]_2(C_4H_4O_6)Cl_2{\cdot}nH_2O$ (Refcode BUDLOB) [80], $Na\{\Delta\text{-}[Fe(bpy)_3]\}_2(C_4H_4O_6)_2Cl{\cdot}14H_2O$ (Refcode BUDLUH) [80], $Na\{\Delta\text{-}[Ru(bpy)_3]\}_2(C_4H_4O_6)_2Cl$ (Refcode BUDMAO) [80], $Na\{\Delta\text{-}[Ni(bpy)_3]\}_2(C_4H_4O_6)_2Cl{\cdot}14H_2O$ (Refcode BUDMES) [80], $[Ru(bpy)_3]_2[Cr(CN)_6]Br{\cdot}8H_2O$ (Refcode HIRDUH) [81], $[Ru(bpy)_3]_2[Cr(CN)_6]Cl{\cdot}8H_2O$

(Refcode HIRFAP) [81] and $[Ru(bpy)_3](N_3)Cl{\cdot}2H_2O$ (Refcode WOYBER) [82] were omitted from the subsequent analysis. A further seven compounds were also omitted as the halide ions were encapsulated within a polyoxometallate anion, $[Ni(bpy)_3]_3[Cl@V_{15}O_{36}]{\cdot}3H_2O$ (Refcode ADOCOM [83], $[Cu(bpy)_3]_3[Cl@V_{15}O_{38}]{\cdot}3H_2O$ (Refcode CEJWEU) [84], $[Cu(bpy)_3]_3[Cl@H_4V_{16}O_{38}]{\cdot}3H_2O$ (Refcode CEJWIY) [84], $[Cd(bpy)_3]_3[Cd(bpy)_2(OH_2)][Cl@V_{16}O_{38}[Cd(bpy)2(OH2)]]{\cdot}1.5H_2O$ (Refcode JETQUV) [85], $[Fe(bpy)_3]_2[Cl@V_{16}O_{38}]{\cdot}4.67H_2O$ (Refcode VUFDAC [86], $[Zn(bpy)_3]_3[Cl@V_{15}O_{36}]{\cdot}3H_2O$ (Refcode WUPWOT) [87] and $[Co(bpy)_3]_3[Cl@V_{15}O_{36}]{\cdot}3H_2O$ (Refcode WUPWUZ) [87], leaving a total of 48 entries for detailed analysis.

### *3.1. The Structural Motifs*

Of the 48 compounds investigated, 20 (41.7%) exhibit an interaction between the halide ion and 12 hydrogen atoms of six 2,2′-bipyridine ligands from six different $[M(bpy)_3]^{n+}$ cations within a sheet, as presented in Figure 2a–c and listed in Table 2. We denote this as Structure Type 1. Apparently, $[Ru(bpy)_3]Cl_2{\cdot}6H_2O$ (Refcode HAXHIZ) [88] adopts Structure Type 1, but unfortunately the disordered water and chloride were removed from the data deposited and no metrical analysis can be made. The halogen and metal centres in the sheet can be co-planar (Figure 3a) or may be ruffled about a mean plane (Figure 3b). An extreme case of ruffling occurs in $\Delta$-$[Co(bpy)_3]Cl_2{\cdot}2H_2O{\cdot}EtOH$ (Refcode CAMHED) in which the six Co atoms deviate by 0.81 to 3.52 Å from the mean plane through them. The metal–metal distances within the six-sided polygon are remarkably similar in the entries listed in Table 2, with a mean value of 7.70(20) Å. One special case deserves mention at this point: in $[Ni(bpy)_3]_2(Hbpy)[Ag_3I_5]I$ (Refcode DUYBIK) [89], the host motif of six $[M(bpy)_3]^{n+}$ cations is maintained, but the iodide is too large to fit in the cavity as a guest and lies above and below the centre. As a result, there are six "normal" H-3 and six longer H-3 interactions with the halide, as well as six additional H-4 interactions (Figure 4a).

The Structure Type 1 arrangement can be disrupted by the presence of other anions, solvent molecules or additional species capable of hydrogen bonding. However, even in such cases, there is a tendency to retain a significant part of the Structure Type 1 motif and the four entries exhibiting this phenomenon are listed in Table 3. The commonest motif is shown in Figure 4b,c and retains three adjacent $[M(bpy)_3]^{n+}$ cations, interacting through atoms H-3 and H-3′ of a bpy from each cation.

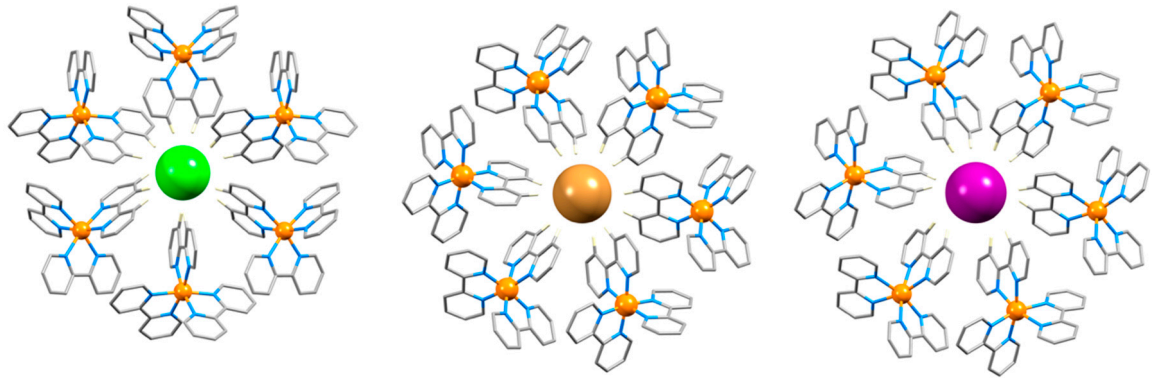

(**a**) (**b**) (**c**)

**Figure 2.** Structure Type 1 with (**a**) chloride ($[Ni(bpy)_3]Cl_2{\cdot}5.5H_2O$, Refcode EGOVEB) [90], (**b**) bromide ($[Fe(bpy)_3]Br_2{\cdot}5.5H_2O$, Refcode IFAFUR) [91] and (**c**) iodide ($[Li(bpy)_3]I{\cdot}bpy$, Refcode REXVOF) [92] ions hosted. Halogen is shown in the space-filling mode, metal atoms in the ball and stick representation and orange, and all the other elements CPK colours. Hydrogen atoms, other than those involved in the interactions with the halide, are omitted.

**Table 2.** Structure Type 1 complexes.

| REFCODE Space Group | X M | H … X/Å | Mean H … X/Å | C … X/Å | Mean C … X/Å | ∠C–H … X/° | Mean ∠C–H … X/° | Ref |
|---|---|---|---|---|---|---|---|---|
| BUDKUG No. 5 | Cl Fe | 2.746–3.057 | 2.849 | 3.809–4.145 | 3.928 | 165.19–179.21 | 172.32 | [80,94] |
| BPNTAR No. 5 | Cl Ni | 2.706–2.9784 | 2.857 | 3.7663–4.0668 | 3.937 | 164.39–178.41 | 172.8 | [95] |
| BUDLIV No. 5 | Cl Co | 2.573–3.236 | 2.904 | 3.596–4.304 | 3.950 | 153.90–172.82 | 162.43 | [80] |
| CAMHED No. 179 | Cl Co | 2.525–2.920 | 2.696 | 3.610–3.989 | 3.771 | 164.97–174.56 | 169.45 | [96] |
| EFOWAA No. 5 | Cl Ni | 2.666–3.074 | 2.819 | 3.729–4.157 | 3.893 | 159.7–177.2 | 169.85 | [97] |
| EGOVEB No. 15 | Cl Ni | 2.777–2.892 | 2.844 | 3.856–3.977 | 3.925 | 170.4–174.6 | 172.0 | [90] |
| IPIMAW No. 5 | Cl Co | 2.699–2.870 | 2.809 | 3.767–3.955 | 3.888 | 166.9–176.3 | 172.1 | [98] |
| HUKWER No. 192 | Cl Ni | 2.9045 | 2.9045 | 3.986 | 3.986 | 172.0 | 172.0 | [99] |
| TIMSOY No. 17 | Cl Ni | 2.736–3.72 | 3.024 | 3.68–4.75 | 4.06 | 144.9–178.6 | 162.5 | [93] |
| XUJQEA * No. 2 | Cl Cu | 2.742–2.974 | 2.845 | 3.828–4.06 | 3.927 | 167.9–177.8 | 173.0 | [100] |
| CIBDOH No. 190 | Br Co | 2.8444–2.8935 | 2.8689 | 3.929–3.982 | 3.955 | 174.2–178.1 | 176.15 | [101] |
| IFAFUR No. 190 | Br Fe | 2.8118–3.0301 | 2.92095 | 3.88–4.12 | 4.00 | 168.4–175.8 | 172.1 | [91] |
| UBIWEK No. 54 | Br Fe | 2.777–2.9177 | 2.8439 | 3.854–4.006 | 3.921 | 167.2–177.8 | 170.9 | [102] |
| UBIXEL No. 54 | Br Ni | 2.7900–2.9307 | 2.8567 | 3.866–4.018 | 3.934 | 167.1–176.4 | 170.85 | [102] |
| UBIXIP No. 54 | Br Co | 2.7860–2.9492 | 2.8562 | 3.853–4.037 | 3.932 | 165.3–176.8 | 170.4 | [102] |
| UBIXOV No. 54 | Br Zn | 2.8000–2.9603 | 2.882 | 3.878–4.048 | 3.959 | 166.7–177.0 | 170.7 | [102] |
| BUCNUK No. 18 | I Ru | 2.936–3.205 | 3.021 | 3.99–4.29 | 4.09 | 160–178 | 170 | [103] |
| DUYBIK † No. 5 | I Ni | 2.899–3.219<br>3.874–4.585 (H-4)<br>3.176–3.618 | 3.083<br>4.247 (H-4)<br>3.421 | 3.797–3.972<br>4.864–5.538 (C-4)<br>3.909–4.127 | 3.885<br>5.227 (C-4)<br>4.037 | 125.8–141.8<br>148.9–155.0 (C-4)<br>112.8–127.7 | 133.4<br>152.2 (C-4)<br>120.6 | [89] |
| REXVOF No. 15 | I Li | 2.947–3.504 | 3.179 | 3.966–4.560 | 4.235 | 155.9–175.1 | 165.4 | [92] |

* The 12 C–H bonds come from four $[Cu(bpy)_3]^{2+}$ cations and two [Cu[py-3,3-(CO2)2](bpy)$_2$] molecules; † The iodide lies above and below the host motif of six cations and exhibits six shorter C–H … I H-3 interactions, six longer with H-3 and also a set of six short C–H … I interactions with the H-4 of the ring with the shorter H-3 interaction.

In total, 24 of the 48 (50%) entries for the $[M(bpy)_3]^{n+}$ complexes with halide anions exhibit short interactions between the halogen and H-3 and H-3′ of the bpy ligands. Furthermore, seven of the nine compounds excluded on the basis that the CSD contains no coordinates (Refcodes BUDLAN, BUDLER, BUDLOB, BUDLUH, BUDMAO, BUDMES and HIRDUH) were all reported as being isostructural with established Structural Type 1 compounds, bringing the total to 31 examples (64.6%).

Another common motif has been identified in nine entries (18.8%) that involve halide ions that are located between sheets containing $[M(bpy)_3]^{n+}$ cations. In this case, the interactions are with only two cations and with three bpy ligands from each cation. However, in contrast to Structure Type 1, the interactions are not with H-3 and H-3′ but rather with an H-5 and H-6 from each ligand (Figure 5a). The distances are typically longer than those observed in Structure Type 1. Nevertheless, the result is

once again 12 C–H . . . halogen interactions but involving only two cations (Figure 5b). Typically, the halide ion also exhibits stronger hydrogen-bonding interactions with water molecules lying in the sheet between the cations. This motif will now be described as Structure Type 2 (Table 4). The interactions with H-6 are typically shorter than those with H-5, but the distances and C–H . . . X angles all indicate that these interactions only represent the weakest of hydrogen bonds and are better described as between a halide guest in a C–H bond-lined host cavity.

**Table 3.** Structure Type 1 sub-motifs with three cations interacting with chloride.

| REFCODE<br>Metal<br>Space Group | H . . . Cl/Å | Mean H<br>. . . Cl/Å | C . . . Cl/Å | Mean C<br>. . . Cl/Å | ∠C–H . . . Cl/° | Mean ∠C–H<br>. . . Cl/° | Ref |
|---|---|---|---|---|---|---|---|
| DIWGIZ<br>Rh<br>No. 62 | 2.516–3.108 | 2.717 | 3.54–4.18 | 3.753 | 151.2–169.5 | 160.5 | [104] |
| CAMHIH<br>Co<br>No. 33 | 2.536–3.119 | 2.752 | 3.605–4.078 | 3.795 | 147.21–178.60 | 164.60 | [96] |
| POMHAB<br>Co<br>No. 64 | 2.463–2.9762 | 2.623 | 3.478–4.047 | 3.692 | 161.1–178.5 | 169.1 | [105] |
| POMHAB01<br>Co<br>No. 64 | 2.4134–2.9391 | 2.601 | 3.463–4.013 | 3.672 | 161.4–178.2 | 169.5 | [106] |

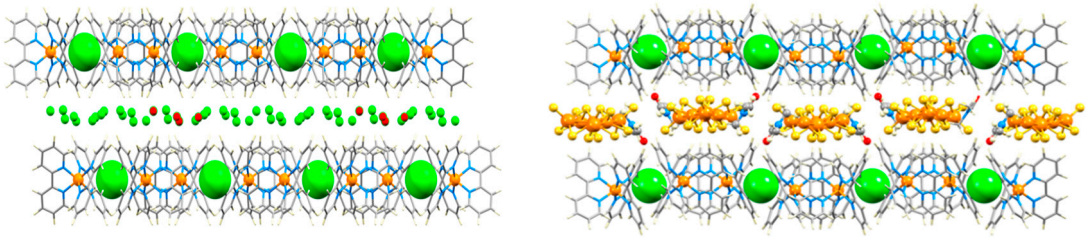

(**a**) (**b**)

**Figure 3.** The Structure Type 1 halide ions are located in a sheet of $[M(bpy)_3]^{n+}$ cations. (**a**) The halogen and metal centres in the sheet can define a plane ($[Ni(bpy)_3]Cl_2{\cdot}5.5H_2O$, Refcode EGOVEB) [90] viewed along *a* or (**b**) the sheet may be ruffled ($[Ni(bpy)_3]_2[Ag_3Mo_3S_{12}]Cl{\cdot}2DMF{\cdot}2H_2O$, Refcode TIMSOY) [93] viewed along *b*). Structure Type 1 halogen shown in space-filling mode, metal atoms and other anions and solvent molecules between the cation sheets as ball and stick representations, metal atoms in orange and all other elements CPK colours. Hydrogen atoms are only shown for the $[M(bpy)_3]^{n+}$ cations.

**Table 4.** Structure Type 2 sub-motifs with twelve C–H . . . X interactions with two cations.

| REFCODE<br>Space Group | X<br>M | H-6 . . . X/Å | Mean<br>H–6 . . . X/Å | H–5 . . . X/Å | Mean<br>H–5 . . . X/Å | Ref |
|---|---|---|---|---|---|---|
| HIGZAY<br>No. 5 | Cl<br>Ru | 3.132–3.497 | 3.320 | 3.327–4.217 | 3.669 | [107] |
| HIRDOB<br>No. 5 | Cl<br>Os | 3.061–3.590 | 3.304 | 3.353–4.110 | 3.700 | [81] |
| HIRDOB01 *,†<br>No. 15 | Cl<br>Os | 3.050–3.749 | 3.421 | 3.484–4.320 | 3.743 | [108] |
| HIRFAP01<br>No. 5 | Cl<br>Ru | 3.145–3.578 | 3.376 | 3.312–4.249 | 3.664 | [109] |

**Table 4.** *Cont.*

| REFCODE Space Group | X M | H-6 . . . X/Å | Mean H–6 . . . X/Å | H–5 . . . X/Å | Mean H–5 . . . X/Å | Ref |
|---|---|---|---|---|---|---|
| INIYIN No. 15 | Cl Ru | 3.140–3.712 | 3.408 | 3.407–4.216 | 3.696 | [110] |
| HIRDUH01 No. 5 | Br Ru | 3.189–3.552 | 3.430 | 3.323–4.091 | 3.678 | [109] |
| ISIMOM No. 33 | I Ga | 3.171–3.443 | 3.326 | 3.796–4.200 | 3.942 | [111] |
| TAHNOG No. 9 | I Ru | 3.141–4.163 | 3.641 | 3.383–4.980 | 3.984 | [112] |
| TAHNOG01 No. 9 | I Ru | 3.108–4.1762 | 3.631 | 3.2959–4.908 | 3.923 | [113] |

* Hydrogen atoms added in normalized positions; † Redetermination and correction of space group for HIRDOB.

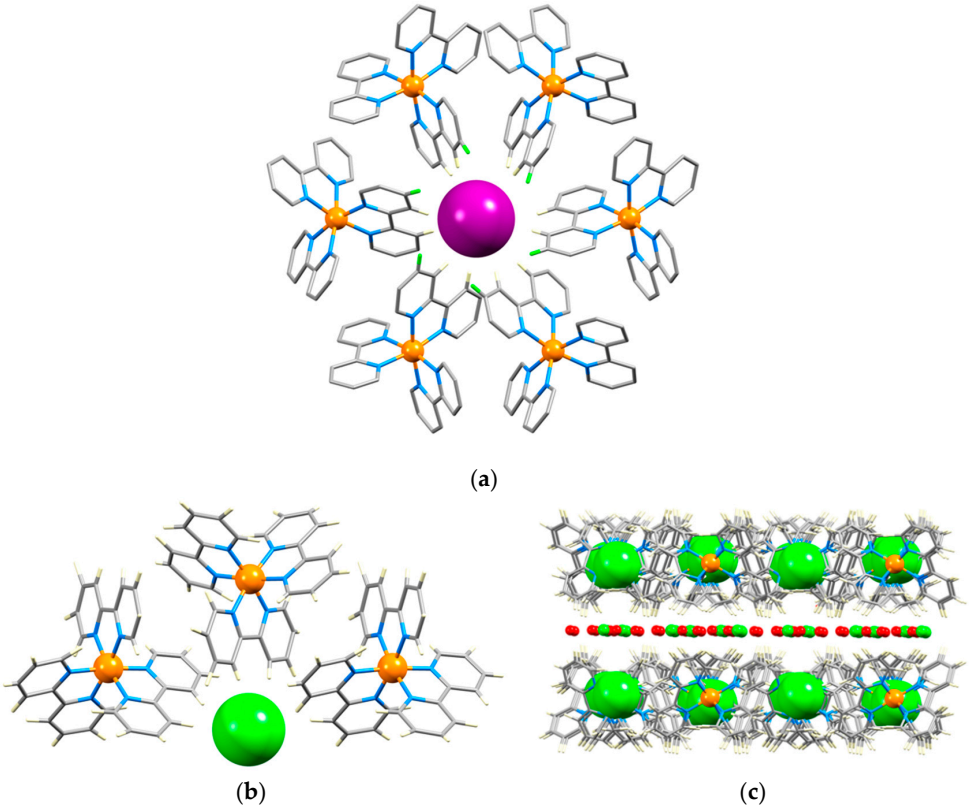

**Figure 4.** The Structure Type 1 motif can persist with fewer interactions with the $[M(bpy)_3]^{n+}$ cations if other anions, solvent molecules or hydrogen bonding species are present. Once again, the halide ions are in a sheet of $[M(bpy)_3]^{n+}$ cations. (**a**) The halide ion does not always lie in the centre of the host constructed from $[M(bpy)_3]^{n+}$ cations. In $[Ni(bpy)_3]_2(Hbpy)[Ag_3I_5]I$ (Refcode DUYBIK) [89], the iodide ions lie above and below the host motif of six cations and each iodide ion exhibits six shorter C–H . . . I H-3 interactions, six longer contacts with H-3 and also a set of six short C–H . . . I interactions with the H-4 of the ring, with a shorter H-3 interaction; hydrogen atoms, other than those involved in interactions with the halide, are omitted and H-4 is shown in green. (**b**) Interactions with three cations result in a set of six H-3 and H-3′ interactions in $[Rh(bpy)_3]Cl_3{\cdot}4H_2O$ (Refcode DIWGIZ) and (**c**) the sheet structure found with just three cations (Refcode DIWGIZ); hydrogen atoms are only shown for the $[M(bpy)_3]^{n+}$ cations. In each figure, Structure Type 1 halide ions are shown in a space-filling mode, metal atoms and other anions and solvent molecules between the cation sheets as ball and stick representations, metal atoms in orange and all other elements CPK colours.

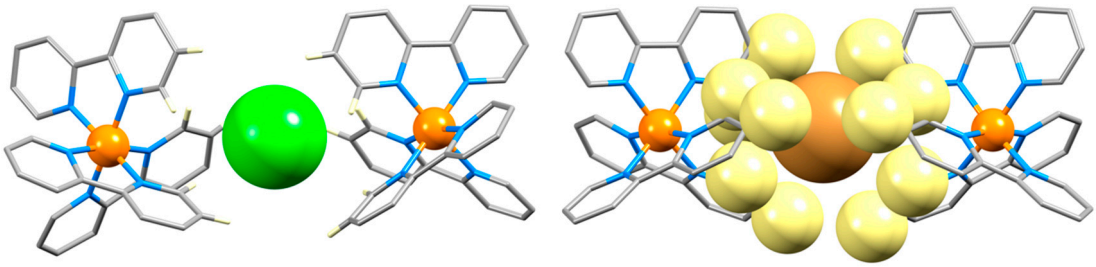

(**a**) (**b**)

**Figure 5.** (**a**) The Structure Type 2 has three bpy ligands of each of the two $[M(bpy)_3]^{n+}$ cations interacting with halide ions located between the sheets of cations, resulting in a set of six H-6 and six H-5 interactions as seen in $[Os(bpy)_3]_2[Cr(CN)_6]Cl{\cdot}8H_2O$ (Refcode HIRDOB) [81]. The halide ion is shown in a space-filling mode, and the metal atoms in ball and stick representations. (**b**) The 12 C–H bonds provide a cavity for the halide guest, as seen in $[Ru(bpy)_3]_2[Cr(CN)_6]Br{\cdot}8H_2O$ (Refcode HIRDUH01) [109]. The Structure Type 2 halide ion and the interacting hydrogens are shown in a space-filling mode, and the metal atoms in ball and stick representations.

### *3.2. A Closer Look at Structure Type 1*

In this section, we look briefly at complexes exhibiting Structure Type 1 and in particular their metrical properties. The detailed analyses were made for the complexes with coordinates in the CSD. In some cases, missing hydrogen atoms were added in normalized positions. All analyses used normalized hydrogen positions. In Figure 2, the archetypical motifs looking down onto the chloride, bromide and iodide ions hosted in the cation sheets were presented, and Figure 6a,b show how the motifs attenuate within the sheet.

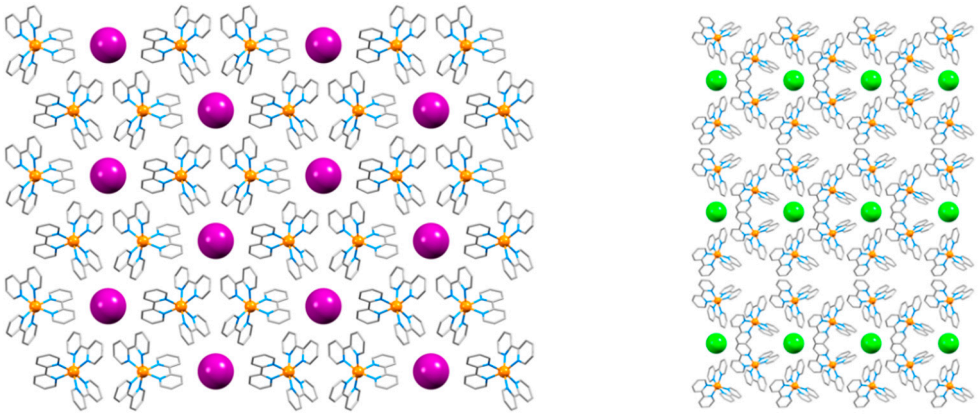

(**a**) (**b**)

**Figure 6.** (**a**) The arrangement of adjacent anions in the typical Structure Type 1 sheet of $([Li(bpy)_3]I{\cdot}bpy$ (Refcode REXVOF) [92]. (**b**) In a variant found in $[Ni(bpy)_3]_2(C_4H_4O_6)Cl_2{\cdot}12H_2O$ (Refcode BPNTAR) [95], alternating rows of halides are missing from the sheets. Halide ions are shown in a space-filling representation, metal atoms (orange) in ball and stick representations and all other elements in CPK colours. Hydrogen atoms are omitted for clarity.

Following the approach of Steiner [114], we present data characterizing the interactions of the halide ions with the cations, hosting them in Tables 2 and 3. The mean H ... Cl and C ... Cl distances are 2.80 Å and 3.87 Å, respectively, and the mean ∠C–H ... Cl is 168.7°; these are slightly longer than the mean distances reported by Steiner for (NN)C($sp^2$)–H ... Cl (2.54, 3.57 Å) and (NC)C($sp^2$)–H ... Cl (2.64, 3.66 Å) [114], although if the increase in mean distance were constant, the expectation values for

(CC)C($sp^2$)–H ... Cl would be 2.74 and 3.75 Å. The mean H ... Br and C ... Br distances are 2.87 Å and 3.95 Å and the mean ∠C–H ... Br is 171.9°; Steiner reports 2.73 and 2.74 Å for H ... Br and 3.72 and 3.74 Å for C ... Br distances in (NN)C($sp^2$)–H ... Br and (NC)C($sp^2$)–H ... Br, respectively. In this case, the expectation values for (CC)C($sp^2$)–H ... Br of H ... Br 2.75 Å and C ... Br 3.78 Å correspond reasonably well to our values. The mean H ... I and C ... I distances are 3.10 Å and 4.16 Å and the mean ∠C–H ... I 167.7°; Steiner reports 2.90 and 2.99 Å for H ... I and 3.85 and 4.00 Å for C ... I distances in (NN)C($sp^2$)–H ... I and (NC)C($sp^2$)–H ... I, respectively. In this case, the expectation values for (CC)C($sp^2$)–H ... I of H ... I 3.08 Å and C ... I 4.15 Å correspond well. The interactions are close to linear and it is reasonable to interpret them in terms of weak hydrogen bonds.

We note that closely related motifs containing functionalized $[M(bpy)_3]^{n+}$ scaffolds are observed in a variety of metallosupramolecular structures [115–118].

### 3.3. An Aside on Chirality

Tris-chelate complexes such as $[M(bpy)_3]^{n+}$ cations are chiral with the metal acting as a stereogenic centre. The absolute configurations of the two enantiomeric forms are denoted as Δ and Λ (Figure 7). Eleven of the entries for Structure Type 1 are enantiopure tartrate compounds: (Λ−$[Ni(bpy)_3]_2(C_4H_4O_6)Cl_2{\cdot}12H_2O$ (Refcode BPNTAR) [95], Λ-$[Ru(bpy)_3]_2(C_4H_4O_6)Cl_2{\cdot}12H_2O$ (Refcode BUDLAN) [80], Λ-$[Fe(bpy)_3]_2(C_4H_4O_6)Br_2{\cdot}11H_2O$ (Refcode BUDLER) [80], Λ-$[Co(bpy)_3]_2(C_4H_4O_6)Cl_2{\cdot}nH_2O$ (Refcode BUDLOB) [80], $Na\{\Delta\text{-}[Fe(bpy)_3]\}_2(C_4H_4O_6)_2Cl{\cdot}14H_2O$ (Refcode BUDLUH) [80], $Na\{\Delta\text{-}[Ru(bpy)_3]\}_2(C_4H_4O_6)_2Cl$ (Refcode BUDMAO) [80], $Na\{\Delta\text{-}[Ni(bpy)_3]\}_2(C_4H_4O_6)_2Cl{\cdot}14H_2O$ (Refcode BUDMES) [80], Δ-$[Ru(bpy)_3]_3[Sb_2(C_4H_2O_6)_2]_2I_2{\cdot}19.5H_2O$ (Refcode BUCNUK) [103], Δ-$[Ni(bpy)_3]_4[Ge_2(C_4H_4O_6)_2(H_2O)_2]Cl_2{\cdot}1.5H_2O$ (Refcode EFOWAA), Λ-$[Fe(bpy)_3]_2(C_4H_4O_6)Cl_2{\cdot}11H_2O$ (Refcode BUDKUG) [80,94] and $Na[Co(bpy)_3]_2(C_4H_4O_6)_2Cl{\cdot}6.5H_2O$ (Refcode BUDLIV [80,94]. These compounds, therefore, contain only cations with the Δ or Λ absolute configurations around the halide.

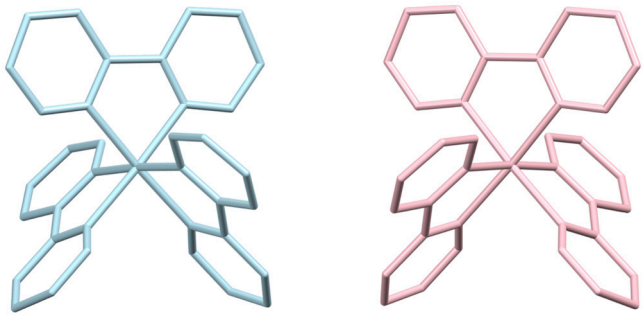

**Figure 7.** IUPAC recommends the notation Δ and Λ for denoting the absolute configuration of octahedral metal complexes. The Δ (pale blue) and Λ (pink) enantiomers of an $[M(bpy)_3]^{n+}$ complex are presented here.

Of the remaining Structure Type 1 compounds, four are found in the Sohncke Space Groups [119] with $[Ni(bpy)_3]_2(Hbpy)[Ag_3I_5]I$ (Space group *C*2, Refcode DUYBIK) [89], $[Ni(bpy)_3]_2[Ag_3Mo_3S_{12}]Cl{\cdot}2DMF{\cdot}2H_2O$ (Space group *P*2221 Refcode TIMSOY) [93] and $[Co(bpy)_3]Cl_2{\cdot}2H_2O{\cdot}EtOH$ (Space group $P6_522$, Refcode CAMHED) [96] all being homochiral. In all of the compounds in non-Sohncke space groups, the cations form homochiral sheets with alternating Δ and Λ chirality (Figure 8). As a result, every halide ion in the Structure Type 1 motif is surrounded by six homochiral $[M(bpy)_3]^{n+}$ cations.

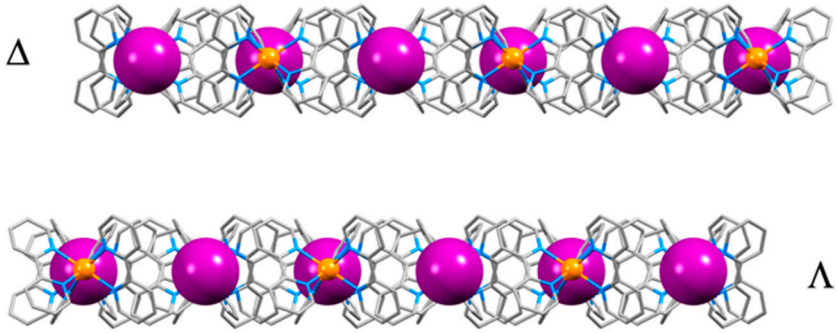


**Figure 8.** Unless the $[M(bpy)_3]^{n+}$ cations in the Structure Type 1 complexes are homochiral, alternating homochiral sheets have opposite Δ and Λ chiralities, as seen in $[Li(bpy)_3]I{\cdot}bpy$ (Refcode REXVOF) [92] (Li, orange; I violet).

### *3.4. From 2,2′-bipyridine to 1,10-phenanthroline*

The chemistry of bpy complexes usually very closely resembles that of the analogous compounds with phen ligands. We wondered whether the packing motifs would be repeated in $[M(phen)_3]^{n+}$ complexes and therefore made a scouting survey of the $[M(phen)_3]^{n+}$ compounds in the CSD. The typical layer structures of the cations were observed in the majority of cases. However, in no case did we find structures analogous to the Type 1 with $[M(bpy)_3]^{n+}$, involving the phen H-5 and H-6 protons. Rather, the halide ions are located between the sheets, with typically Type 2 interactions involving phen H-2(9) and H-3(8). This observation also confirms our belief that Structure Type 1 involves direct C–H … X interactions rather than a simple host–guest binding in a cavity.

## 4. Conclusions

We have carried out a detailed analysis of the interactions between homoleptic 2,2′-bipyridine metal complexes $[M(bpy)_3]^{n+}$ and halide ions in the solid state. Two recurring packing motifs are found among the 48 compounds investigated. Structure Type I comprises an interaction between a halide ion and 12 hydrogen atoms of six 2,2′-bipyridine ligands from six different $[M(bpy)_3]^{n+}$ cations within a sheet. This motif involves the H-3 and H-3′ of each bpy ligand. The Structure Type 1 motif may persist with fewer than six bpy ligands if other anions, solvent molecules or hydrogen-bond donors are present. Structure Type 2 involves halide ions located between sheets of the $[M(bpy)_3]^{n+}$ cations; in this motif, three bpy ligands of each of the two $[M(bpy)_3]^{n+}$ cations interact with the halide ions positioned between the sheets of cations, resulting in a set of six H-6 and six H-5 interactions.

**Author Contributions:** Conceptualization, E.C.C. and C.E.H.; methodology, E.C.C.; formal analysis, E.C.C.; writing—original draft preparation, E.C.C.; writing—review and editing, E.C.C. and C.E.H. Both authors have read and agreed to the published version of the manuscript.

**Funding:** This research was partially funded by the Swiss National Science Foundation (grant number 200020_182559).

**Acknowledgments:** We thank the University of Basel and the Swiss National Science Foundation for ongoing support.

**Conflicts of Interest:** The authors declare no conflict of interest.

## References

1. ICSD FIZ Karlsruhe–Leibnitz Institute for Information Infrastructure. Available online: https://www.european-mrs.com/fiz-karlsruhe-%E2%80%93-leibniz-institute-information-infrastructure (accessed on 20 March 2020).
2. NIST Inorganic Crystal Structure Database, NiISTStandard Reference Database Number 3, National Institute of Standards and Technology, Gaithersburg Md, 20899. Available online: https://www.nist.gov/programs-projects/crystallographic-databases (accessed on 20 March 2020).

3. PDBE Protein Data Bank in Europe. Available online: https://www.ebi.ac.uk/pdbe/ (accessed on 20 March 2020).
4. RCSB Protein Data Bank. Available online: https://www.rcsb.org (accessed on 20 March 2020).
5. PDBJ Protein Data Bank Japan. Available online: https://pdbj.org (accessed on 20 March 2020).
6. CCDC the Cambridge Structural Database (CSD). Available online: https://www.ccdc.cam.ac.uk (accessed on 20 March 2020).
7. Groom, C.R.; Bruno, I.J.; Lightfoot, M.P.; Ward, S.C. The Cambridge Structural Database. *Acta Crystallogr.* **2016**, *72B*, 171–179. [CrossRef] [PubMed]
8. Macrae, C.F.; Sovago, I.; Cottrell, S.J.; Galek, P.T.A.; McCabe, P.; Pidcock, E.; Platings, M.; Shields, G.P.; Stevens, J.S.; Towler, M.; et al. Mercury 4.0: From visualization to analysis, design and prediction. *J. Appl. Crystallogr.* **2020**, *53*, 226–235. [CrossRef] [PubMed]
9. Bruno, I.J.; Cole, J.C.; Edgington, P.R.; Kessler, M.; Macrae, C.F.; McCabe, P.; Pearson, J.; Taylor, R. New software for searching the Cambridge Structural Database and visualizing crystal structures. *Acta Crystallogr.* **2002**, *58B*, 389–397. [CrossRef] [PubMed]
10. Schneider, G.E.; Bolink, H.J.; Constable, E.C.; Ertl, C.D.; Housecroft, C.E.; Pertegàs, A.; Zampese, J.A.; Kanitz, A.; Kessler, F.; Meier, S.B. Chloride ion impact on materials for light-emitting electrochemical cells. *Dalton Trans.* **2014**, *43*, 1961–1964. [CrossRef] [PubMed]
11. Constable, E.C.; Housecroft, C.E. More Hydra than Janus—Non-classical coordination modes in complexes of oligopyridine ligands. *Coord. Chem. Rev.* **2017**, *350*, 84–104. [CrossRef]
12. Constable, E.C.; Seddon, K.R. A deuterium exchange reaction of the tris-(2,2′-bipyridine)ruthenium(II) cation: Evidence for the acidity of the 3,3′-protons. *J. Chem. Soc. Chem. Commun.* **1982**, 34–36. [CrossRef]
13. Constable, E.C.; Lewis, J. Nmr studies on ruthenium(ii) α,α′-diimine complexes; further evidence for unique reactivity at H3,3′ of coordinated 2,2′-bipyridines. *Inorg. Chim. Acta* **1983**, *70*, 251–253. [CrossRef]
14. McClanahan, S.; Hayes, T.; Kincaid, J. Resonance Raman spectra of the ground and excited states of specifically deuterated tris(2,2′-bipyridine)ruthenium(II). *J. Am. Chem. Soc.* **1983**, *105*, 4486–4487. [CrossRef]
15. McClanahan, S.; Kincaid, J. Vibrational spectra of specifically deuteriated 2,2′-bipyridine complexes of Fe(II), Ru(II) and Os(II). *J. Raman Spectrosc.* **1984**, *15*, 173–178. [CrossRef]
16. McClanahan, S.F.; Kincaid, J.R. $^{3}$MLCT lifetimes of tris(2,2′-bipyridine)ruthenium(II). Position-dependent deuterium effects. *J. Am. Chem. Soc.* **1986**, *108*, 3840–3841. [CrossRef]
17. Wernberg, O. A kinetic investigation of the base-catalysed deuterium-exchange reaction of tris(2,2′-bipyridine)osmium(II) ion in dimethyl sulphoxide solution. *J. Chem. Soc. Dalton Trans.* **1986**, 1993–1994. [CrossRef]
18. Constable, E.C. Ligand reactivity in 2,2′-bipyridine complexes; charge effects upon reactions with base. *Polyhedron* **1989**, *8*, 83–86. [CrossRef]
19. Butschke, B.; Schwarz, H. "Rollover" cyclometalation—Early history, recent developments, mechanistic insights and application aspects. *Chem. Sci.* **2012**, *3*, 308–326. [CrossRef]
20. Desiraju, G.R.; Steiner, T. *The Weak Hydrogen Bond: In Structural Chemistry and Biology*; Oxford University Press: Oxford, UK, 1999.
21. Broder, C.K.; Davidson, M.G.; Forsyth, V.T.; Howard, J.A.K.; Lamb, S.; Mason, S.A. On the reliability of C−H···O interactions in crystal engineering: synthesis and structure of two hydrogen bonded phosphonium bis(aryloxide) salts. *Cryst. Growth Des.* **2002**, *2*, 163–169. [CrossRef]
22. Desiraju, G.R. *The Crystal as a Supramolecular Entity*; Wiley: Chichester, UK, 1996.
23. Brandt, W.W.; Dwyer, F.P.; Gyarfas, E.D. Chelate complexes of 1,10-phenanthroline and related compounds. *Chem. Rev.* **1954**, *54*, 959–1017. [CrossRef]
24. Constable, E.C. The coordination chemistry of 2,2′:6′,2″-terpyridine and higher oligopyridines. *Adv. Inorg. Chem.* **1986**, *30*, 69–121. [CrossRef]
25. Constable, E.C. Homoleptic complexes of 2,2′-bipyridine. *Adv. Inorg. Chem.* **1989**, *34*, 1–63. [CrossRef]
26. Constable, E.C.; Housecroft, C.E. The early years of 2,2′-bipyridine—A ligand in its own lifetime. *Molecules* **2019**, *24*, 3951. [CrossRef]
27. Constable, E.C. 2,2′:6′,2″-terpyridines: From chemical obscurity to common supramolecular motifs. *Chem. Soc. Rev.* **2007**, *36*, 246–253. [CrossRef]
28. Constable, E.C. Higher oligopyridines as a structural motif in metallosupramolecular chemistry. *Prog. Inrog. Chem.* **1994**, *42*, 67–138. [CrossRef]

29. Constable, E.C.; Housecroft, C.E. 'Simple' oligopyridine complexes—Sources of unexpected structural diversity. *Aust. J. Chem.* **2020**, *73*, 390. [CrossRef]
30. Fallahpour, R.-A. The higher oligopyridines and their metal complexes. *Curr. Org. Synth.* **2006**, *3*, 19–39. [CrossRef]
31. Kaes, C.; Katz, A.; Hosseini, M.W. Bipyridine: The most widely used ligand. A review of molecules comprising at least two 2,2′-bipyridine units. *Chem. Rev.* **2000**, *100*, 3553–3590. [CrossRef] [PubMed]
32. Lindoy, L.F.; Livingstone, S.E. Complexes of iron(II), cobalt(II) and nickel(II) with α-diimines and related bidentate ligands. *Coord. Chem. Rev.* **1967**, *2*, 173–193. [CrossRef]
33. Schubert, U.S.; Hofmeier, H.; Newkome, G.R. *Modern Terpyridine Chemistry*; Wiley: Weinheim, Germany, 2006.
34. Schubert, U.S.; Winter, A.; Newkome, G.R. *Terpyridine-Based Materials*; Wiley-VCH Verlag GmbH & Co. KGaA: Weinheim, Germany, 2011.
35. Summers, L.A. The bipyridines. *Adv. Heterocycl. Chem.* **1984**, *35*, 281–374. [CrossRef]
36. McWhinnie, W.R.; Miller, J.D. The chemistry of complexes containing 2,2′-bipyridyl, 1,10-phenanthroline, or 2,2′,6′,2″-terpyridyl as ligands. *Adv. Inorg. Chem. Radiochem.* **1970**, *12*, 135–215. [CrossRef]
37. Constable, E.C. A journey from solution self-assembly to designed interfacial assembly. *Adv. Inorg. Chem.* **2018**, *71*, 79–134. [CrossRef]
38. Constable, E.C. Metallosupramolecular chemistry. *Chem. Ind.* **1994**, 56–59.
39. Glasson, C.R.K.; Lindoy, L.F.; Meehan, G.V. Recent developments in the d-block metallo-supramolecular chemistry of polypyridyls. *Coord. Chem. Rev.* **2008**, *252*, 940–963. [CrossRef]
40. Steel, P.J. Metallosupramolecular chemistry—What is it? *ChemInform* **2004**, *35*. [CrossRef]
41. Dance, I.; Scudder, M. Supramolecular motifs: Sextuple aryl embraces in crystalline $[M(2,2'\text{-bipy})_3]$ and related complexes. *J. Chem. Soc. Dalton Trans.* **1998**, 1341–1350. [CrossRef]
42. McMurtrie, J.; Dance, I. Alternative two-dimensional embrace nets formed by metal complexes of 4′-phenylterpyridine crystallised with hydrophilic anions. *CrystEngComm* **2010**, *12*, 3207–3217. [CrossRef]
43. McMurtrie, J.; Dance, I. Crystal packing in metal complexes of 4′-phenylterpyridine and related ligands: Occurrence of the 2D and 1D terpy embrace arrays. *CrystEngComm* **2009**, *11*, 1141–1149. [CrossRef]
44. McMurtrie, J.; Dance, I. Alternative metal grid structures formed by $[M(terpy)_2]^{2+}$ and $[M(terpyOH)_2]^{2+}$ complexes with small and large tetrahedral dianions, and by $[Ru(terpy)_2]^0$. *CrystEngComm* **2010**, *12*, 2700–2710. [CrossRef]
45. Dance, I. Intermolecular embraces and intermolecular energies. *Mol. Cryst. Liq. Cryst.* **2005**, *440*, 265–293. [CrossRef]
46. Maharaj, F.; Russell, V.; Chow, H.; Page, M.; Scudder, M.; Craig, D.; Dance, I. Polymorphs and pseudo-polymorphs: Nine crystals containing $[Fe(phen)_3]^{2+}$ associated with $[HgI_4]^{2-}$. *CrystEngComm* **2003**, *5*, 285–293. [CrossRef]
47. McMurtrie, J.; Dance, I. Engineering grids of metal complexes: Development of the 2D $M(terpy)_2$ embrace motif in crystals. *CrystEngComm* **2005**, *7*, 216–229. [CrossRef]
48. McMurtrie, J.; Dance, I. Engineering the metal-terpy grid with complexes containing 4′-hydroxy terpyridine. *CrystEngComm* **2005**, *7*, 230–236. [CrossRef]
49. Dance, I. Inorganic intermolecular motifs, and their energies. *CrystEngComm* **2003**, *5*, 208–221. [CrossRef]
50. Dance, I. Distance criteria for crystal packing analysis of supramolecular motifs. *New J. Chem.* **2003**, *27*, 22–27. [CrossRef]
51. Maharaj, F.; Russell, V.; Scudder, M.; Craig, D.; Dance, I. A highly symmetric lattice of tightly packed supramolecular interactions of $[Fe(phen)_3]^{2+}$ with $[HgI_3]^-$, $[ClHgI_3]^{2-}$, and $Cl^-$. *CrystEngComm* **2002**, *4*, 149–154. [CrossRef]
52. Horn, C.; Berben, L.; Chow, H.; Scudder, M.; Dance, I. Supramolecular motifs in four pseudo-polymorphic crystals of $[Fe(phen)_3](I_3)_2\cdot$(solvent): Solvent = acetone, $CH_2Cl_2$, $CH_3CN$, toluene or $H_2O$. *CrystEngComm* **2002**, *4*, 7–12. [CrossRef]
53. Horn, C.; Scudder, M.; Dance, I. Crystal structures, crystal packing and supramolecular motifs in $[Fe(phen)_3]I_{14}$ and $[M(phen)_3]I_{18}$ (M⊕=⊕Fe, Ni): Complementary orthogonality of $[M(phen)_3]^{2+}$ cations and polyiodide anions. *CrystEngComm* **2001**, *3*, 9–14. [CrossRef]
54. Horn, C.; Scudder, M.; Dance, I. Contrasting crystal supramolecularity for $[Fe(phen)_3]I_8$ and $[Mn(phen)_3]I_8$: Complementary orthogonality and complementary helicity. *CrystEngComm* **2001**, *3*, 1–8. [CrossRef]

55. Horn, C.; Scudder, M.; Dance, I. The crystal packing of $[M(phen)_3]I_7$ (M = Mn, Fe). *CrystEngComm* **2000**, *2*, 196–200. [CrossRef]
56. Russell, V.; Scudder, M.; Dance, I. The crystal supramolecularity of metal phenanthroline complexes. *Dalton Trans.* **2001**, 789–799. [CrossRef]
57. Horn, C.; Scudder, M.; Dance, I. Crystal supramolecular motifs in trimorphs of $[Fe(phen)_3]I_{12}$. *CrystEngComm* **2000**, *2*, 53–66. [CrossRef]
58. Horn, C.; Ali, B.; Dance, I.; Scudder, M.; Craig, D. Crystal supramolecularity: Extended aryl embraces in dimorphs of $[Cu(1,10\text{-phen})_2I]I_3$. *CrystEngComm* **2000**, *2*, 6–15. [CrossRef]
59. Nassimbeni, L.R.; Bond, D.R.; Moore, M.; Papanicolaou, S. Structure-energy relationships of Werner clathrates. *Acta Crystallogr.* **1984**, *40A*, C111. [CrossRef]
60. Noa, F.M.A.; Bourne, S.A.; Nassimbeni, L.R. Hydrogen bonding and secondary interactions in halogenated complexes. *Acta Crystallogr.* **2017**, *73A*, C736. [CrossRef]
61. Noa, F.M.A.; Bourne, S.A.; Su, H.; Weber, E.; Nassimbeni, L.R. Hydrogen bonding versus halogen bonding in host guest compounds. *Cryst. Growth Des.* **2016**, *16*, 4765–4771. [CrossRef]
62. Noa, F.M.A.; Bourne, S.A.; Su, H.A.; Nassimbeni, L.R. Secondary interactions in halogenated Werner clathrates. *Cryst. Growth Des.* **2017**, *17*, 1876–1883. [CrossRef]
63. Sykes, N.M.; Su, H.; Bourne, S.A.; Nassimbeni, L.R. Enclathration by Werner hosts: Selectivity and polymorphism. *Cryst. Growth Des.* **2020**, *20*, 274–280. [CrossRef]
64. Wicht, M.; Bathori, N.; Nassimbeni, L. Mixed-ligand Ni–Werner complexes: Enhanced selectivity and hydrogen bonding frameworks. *Acta Crystallogr.* **2018**, *74A*, E130. [CrossRef]
65. Wicht, M.M.; Nassimbeni, L.R.; Bathori, N.B. Werner clathrates with enhanced hydrogen bonding functionality. *Polyhedron* **2019**, *163*, 7–19. [CrossRef]
66. Beck, M.T. Chemistry of the outer-sphere complexes. *Coord. Chem. Rev.* **1968**, *3*, 91–115. [CrossRef]
67. Eaton, D.R. Outer sphere complexes as intermediates in coordination chemistry. *Rev. Chem. Intermed.* **1988**, *9*, 201–232. [CrossRef]
68. Bizunok, M.B.; Pyartman, A.K.; Mironov, V.E. Interaction of tris(2,2′-dipyridylchromium(III)) with chloride-, bromide-, nitrate-, iodide-, and sulfate ions in aqueous solutions. *Izv. Vyssh. Uchebn. Zaved. Khim. Khim. Tekhnol.* **1983**, *26*, 907–910.
69. Chattopadhyay, P.K.; Coetzee, J.F. Influence of anionic inner-sphere substituents on the kinetics of ternary complex formation of nickel(II) in acetonitrile as solvent. Opposing effects of solvent labilization and outer-sphere destabilization. *Inorg. Chem.* **1976**, *15*, 400–405. [CrossRef]
70. Coetzee, J.F.; Gilles, D.M. Binary and ternary complex formation of nickel(II) in methanol. Further evidence for outer-sphere stabilization and other factors contributing to ligand substitution kinetics in nonaqueous solvents. *Inorg. Chem.* **1976**, *15*, 405–408. [CrossRef]
71. Fox, D.; Wells, C.F. Kinetics of the oxidation of chloride ions by tris(2,2′-bipyridine)nickel(III) ions in aqueous perchlorate media. *J. Chem. Soc. Dalton Trans.* **1989**, 151–154. [CrossRef]
72. Kameta, N.; Imura, H.; Ohashi, K. Stability constants of inner- and outer-sphere complexes of hydrated tris(1-(2-thienyl)-4,4,4-trifluoro-1,3-butanedionato) lanthanide(III) with tris(2,4-pentanedionato) cobalt(III). *Polyhedron* **2002**, *21*, 805–810. [CrossRef]
73. Ilcheva, L.; Beck, M.T. Effect of ionic strength on the stability of outer sphere complexes. *Magy. Kem. Foly.* **1974**, *80*, 132–135.
74. Ilcheva, L.; Beck, M.T. The effect of ionic strength on the stability outer sphere complexes. *Acta Chim. Acad. Sci. Hung.* **1978**, *97*, 45–49.
75. Johansson, L. Outer-sphere complexes of the tris(1,10-phenanthroline)iron(II) and tris(2,2′-bipyridine)iron(II) ions with several anions. *Chem. Scr.* **1976**, *10*, 72–75.
76. Langford, C.H.; Vuik, C.P.J.; Kane-Maguire, N.A.P. Ligand field redox photochemistry of phenanthroline and bipyridine cobalt(III) complexes. Oxalate as an inner and outer sphere reducing agent. *Inorg. Nucl. Chem. Lett.* **1975**, *11*, 377–380. [CrossRef]
77. Pyartman, A.K.; Gromova, G.I.; Mironov, V.E. Reactions of mixed complexing and substitution of ligands in the second sphere of tris(2,2′-dipyridyl)iron(II). Halide compounds. *Koord. Khim.* **1980**, *6*, 443–445.
78. Pyartman, A.K.; Gromova, G.I.; Mironov, V.E. Reactions of mixed complexing and substitution of ligands in the second sphere of tris(2,2′-dipyridyl)iron(II). Perchlorate-halide compounds. *Koord. Khim.* **1980**, *6*, 439–442.

79. Pov-Ray. Available online: http://www.povray.org (accessed on 20 March 2020).
80. Tada, T. Optical resolution of tris(2,2′-bipyridine)metal(II) by *d*-tartrate. *J. Sci. Hiroshima Univ. Ser. A Phys. Chem.* **1982**, *46*, 73–93.
81. Otsuka, T.; Takahashi, N.; Fujigasaki, N.; Sekine, A.; Ohashi, Y.; Kaizu, Y. Crystal structure and energy transfer in double-complex salts composed of tris(2,2′-bipyridine)ruthenium(II) or tris(2,2′-bipyridine)osmium(II) and hexacyanochromate(III). *Inorg. Chem.* **1999**, *38*, 1340–1347. [CrossRef]
82. Wang, W.-Z.; Liu, X.; Liao, D.-Z.; Jiang, Z.-H.; Yan, S.-P.; Yao, X.-K.; Wang, G.-L. A novel complex of sandwich layers having disordered symbiotic distribution of azido group and water molecules. *Inorg. Chem. Comm.* **2001**, *4*, 416–418. [CrossRef]
83. Zhang, C.-D.; Liu, S.-X.; Gao, B.; Sun, C.-Y.; Xie, L.-H.; Yu, M.; Peng, J. Hybrid materials based on metal–organic coordination complexes and cage-like polyoxovanadate clusters: Synthesis, characterization and magnetic properties. *Polyhedron* **2007**, *26*, 1514–1522. [CrossRef]
84. Dong, B.; Peng, J.; Chen, Y.; Kong, Y.; Tian, A.; Liu, H.; Sha, J. Ph-controlled assembly of two polyoxovanadates based on $[V_{16}O_{38}(Cl)]^{8-}$ and $[V_{15}O_{36}(Cl)]^{6-}$ building blocks. *J. Mol. Struct.* **2006**, *788*, 200–205. [CrossRef]
85. Dong, B.; Peng, J.; Tian, A.; Sha, J.; Li, L.; Liu, H. Two new inorganic–organic hybrid single pendant hexadecavanadate derivatives with bifunctional electrocatalytic activities. *Electrochim. Acta* **2007**, *52*, 3804–3812. [CrossRef]
86. Shi, S.-Y.; Chen, Y.; Liu, B.; Lu, Y.-K.; Xu, J.-N.; Cui, X.-B.; Xu, J.-Q. Two supramolecular compounds based on cage-like polyoxovanadates: Syntheses, crystal structures, and characterizations. *J. Coord. Chem.* **2009**, *62*, 2937–2948. [CrossRef]
87. Li, Y.-G.; Lu, Y.; Luan, G.-Y.; Wang, E.-B.; Duan, Y.-B.; Hu, C.-W.; Hu, N.-H.; Jia, H.-Q. Hydrothermal syntheses and crystal structures of new cage-like mixed-valent polyoxovanadates. *Polyhedron* **2002**, *21*, 2601–2608. [CrossRef]
88. Low, K.S.; Cole, J.M.; Zhou, X.; Yufa, N. Rationalizing the molecular origins of Ru- and Fe-based dyes for dye-sensitized solar cells. *Acta Crystallogr.* **2012**, *68B*, 137–149. [CrossRef]
89. Lei, X.W.; Yue, C.Y.; Zhao, J.Q.; Han, Y.F.; Yang, J.T.; Meng, R.R.; Gao, C.S.; Ding, H.; Wang, C.Y.; Chen, W.D.; et al. Two types of 2d layered iodoargentates based on trimeric $[Ag_3I_7]$ secondary building units and hexameric $[Ag_6I_{12}]$ ternary building units: Syntheses, crystal structures, and efficient visible light responding photocatalytic properties. *Inorg. Chem.* **2015**, *54*, 10593–10603. [CrossRef]
90. Ruiz-Pérez, C.; Lorenzo Luis, P.A.; Lloret, F.; Julve, M. Dimensionally controlled hydrogen-bonded nanostructures: Synthesis, structure, thermal and magnetic behaviour of the tris-(chelated)nickel(II) complex $[Ni(bipy)_3Cl_2{\cdot}5.5H_2O$ (bipy = 2,2′-bipyridyl). *Inorg. Chim. Acta* **2002**, *336*, 131–136. [CrossRef]
91. Heilmann, J.; Lerner, H.-W.; Bolte, M. Tris(2,2′-bipyridyl)iron(II) dibromide 4.5-hydrate. *Acta Crystallogr* **2006**, *62E*, m1477–m1478. [CrossRef]
92. Fischer, E.; Hummel, H.-U. Untersuchungen im quasi-binären System LiI/2,2′-Bipyridin. *Z. Anorg. Allgem. Chem.* **1997**, *623*, 483–486. [CrossRef]
93. Cao, Y.; Zhang, J.-F.; Bei, F.-L.; Zhang, C.; Yang, J.-Y.; Song, Y.-L. Two new configurations of 1-d heterothiometallic clusters: Isomerism of polymeric anions induced by both complementary cations and anions. *Inorg. Chem. Comm.* **2007**, *10*, 1214–1217. [CrossRef]
94. Tada, T.; Kushi, Y.; Yoneda, H. Three types of diastereomeric salts containing tris-(2,2′-bipyridine)metal(II) complex and d-tartrate ions. *Inorg. Chim. Acta* **1982**, *64*, L243–L245. [CrossRef]
95. Wada, A.; Katayama, C.; Tanaka, J. The crystal structure and absolute configuration of $(+)_{589}$-tris(2,2′-bipyridyl)nickel(II) chloride $(+)_{589}$-tartrate hydrate, $[Ni(C_{10}H_8N_2)_3]_2Cl_2.C_4H_4O_6.nH2O$. *Acta Crystallogr.* **1976**, *32B*, 3194–3199. [CrossRef]
96. Szalda, D.J.; Creutz, C.; Mahajan, D.; Sutin, N. Electron-transfer barriers and metal-ligand bonding as a function of metal oxidation state. 2. Crystal and molecular structures of tris(2,2′-bipyridine)cobalt(II) dichloride-2-water-ethanol and tris(2,2′-bipyridine)cobalt(I) chloride-water. *Inorg. Chem.* **1983**, *22*, 2372–2379. [CrossRef]
97. Seifullina, I.; Martsinko, E.; Chebanenko, E.; Afanasenko, E.; Dyakonenko, V.; Shishkina, S. Supramolecular organization and structure of Cu(II) and Ni(II), 2,2′-bipyridine cations with tartratogermanate anions. *Polyhedron* **2019**, *169*, 261–265. [CrossRef]
98. Sun, J.; Xu, H. Supramolecular assembly of $[Co_2(2,2'\text{-bpy})_6]{\cdot}(BTCA){\cdot}Cl{\cdot}11H_2O$: 3D negatively charged cages. *Inorg. Chem. Comm.* **2011**, *14*, 254–257. [CrossRef]

99. Wood, P.A.; Scott, R.; Brechin, E. CSD Communication, 2015. (CCDC 1418045).
100. Doğan, D.; Çolak, A.T.; Şahin, O.; Tunç, T.; Çelik, Ö. The syntheses, crystal structures, spectroscopic and thermal characterization of new pyridine-2,5-dicarboxylate compounds. *Polyhedron* **2015**, *93*, 37–45. [CrossRef]
101. Papadopoulos, C.D.; Hatzidimitriou, A.G.; Voutsas, G.P.; Lalia-Kantouri, M. Synthesis and characterization of new addition compounds of bis(substituted-salicylaldehydo) cobalt(II) with 2,2′-bipyridine (bipy). Crystal and molecular structures of $[Co^{II}$(3-methoxy-salicylaldehyde$)_2$(bipy)]·$CH_3OH$ (**1**) and $[Co^{II}(bipy)_3]Br_2$·0.5(5-chloro-salicylaldehydeH)·1.5$CH_3OH$ (**5**). *Polyhedron* **2007**, *26*, 1077–1086. [CrossRef]
102. Yue, C.Y.; Lei, X.W.; Han, Y.F.; Lu, X.X.; Tian, Y.W.; Xu, J.; Liu, X.F.; Xu, X. Transition-metal-complex cationic dyes photosensitive to two types of 2d layered silver bromides with visible-light-driven photocatalytic properties. *Inorg. Chem.* **2016**, *55*, 12193–12203. [CrossRef]
103. Puttreddy, R.; Hutchison, J.A.; Gorodetski, Y.; Harrowfield, J.; Rissanen, K. Enantiomer separation of tris(2,2′-bipyridine)ruthenium(II): Interaction of a $D_3$-symmetric cation with a $C_2$-symmetric anion. *Cryst. Growth Des.* **2015**, *15*, 1559–1563. [CrossRef]
104. Hubesch, B.; Mahieu, B.; Meunier-Piret, J. Médiation électronique et effet de température dans le cycle photocatalytique du tris(2,2′-bipyridine)rhodium(III). *Bull. Soc. Chim. Belg.* **2010**, *94*, 685–696. [CrossRef]
105. Liu, W.; Xu, W.; Lin, J.L.; Xie, H.Z. Tris(2,2′-bipyridine-κN:N′)cobalt(III) trichloride tetra-hydrate. *Acta Crystallogr.* **2008**, *64E*, m1586. [CrossRef]
106. Casado, F.J.M.; Riesco, M.R. CSD Communication, 2010. (CCDC 768832).
107. Tamura, H.; Ikeda, N.; Iguro, T.; Ohno, T.; Matsubayashi, G.E. The pseudo-racemic complex bis[tris(2,2′-bipyridine)ruthenium(II)] hexacyanocobaltate(III) chloride octahydrate, $[Ru(bpy)_3]_2[Co(CN)_6]Cl.8H_2O$. *Acta Crystallogr.* **1996**, *52C*, 1394–1399. [CrossRef]
108. Marsh, R.E.; Spek, A.L. Use of software to search for higher symmetry: Space group *C*2. *Acta Crystallogr.* **2001**, *57B*, 800–805. [CrossRef] [PubMed]
109. Otsuka, T.; Sekine, A.; Fujigasaki, N.; Ohashi, Y.; Kaizu, Y. Energy-transfer rate in crystals of double-complex salts composed of $[Ru(N\text{-}N)_3]^{2+}$ (N-N = 2,2′-bipyridine or 1,10-phenanthroline) and $[Cr(CN)_6]^{3-}$: Effect of relative orientation between donor and acceptor. *Inorg. Chem.* **2001**, *40*, 3406–3412. [CrossRef]
110. Sakai, K.; Uchida, Y.; Kajiwara, T.; Ito, T. Bis[tris(2,2′-bipyridine-kappa2N,N′)ruthenium(II)] hexacyanoferrate(III) chloride octahydrate. *Acta Crystallogr.* **2004**, *60C*, m65–m68. [CrossRef]
111. Baker, R.J.; Jones, C.; Kloth, M.; Mills, D.P. The reactivity of gallium(I) and indium(I) halides towards bipyridines, terpyridines, imino-substituted pyridines and bis(imino)acenaphthenes. *New J. Chem.* **2004**, *28*, 207–213. [CrossRef]
112. Dong, W.; Shu-Feng, S.I.; Liao, D.-Z.; Jiang, Z.-H.; Yan, S.-P. Syntheses and crystal structures of two ion pair complexes, $[Ru(bpy)_3]_2[Fe(CN)_6]I\cdots 7H_2O$ and $[Ru(bpy)_3][Fe(CN)_5NO]CH_3OH\cdots H_2O$. *J. Coord. Chem.* **2003**, *56*, 531–538. [CrossRef]
113. Dong, W.; Ou-Yang, Y.; Song, H.-B.; Liao, D.-Z.; Jiang, Z.-H.; Yan, S.-P.; Cheng, P. Structure of an $I^-\cdot(H_2O)_6$ anion cluster in a 3D anion crystal host $[I\cdot(H_2O)_6Fe(CN)_6\cdot H_2O]_4$. *Inorg. Chem.* **2006**, *45*, 1168–1172. [CrossRef] [PubMed]
114. Steiner, T. Hydrogen-bond distances to halide ions in organic and organometallic crystal structures: Up-to-date database study. *Acta Crystallogr.* **1998**, *54B*, 456–463. [CrossRef]
115. Marcos, V.; Stephens, A.J.; Jaramillo-Garcia, J.; Nussbaumer, A.L.; Woltering, S.L.; Valero, A.; Lemonnier, J.F.; Vitorica-Yrezabal, I.J.; Leigh, D.A. Allosteric initiation and regulation of catalysis with a molecular knot. *Science* **2016**, *352*, 1555–1559. [CrossRef]
116. Hasenknopf, B.; Lehn, J.-M.; Kneisel, B.O.; Baum, G.; Fenske, D. Self-assembly of a circular double helicate. *Angew. Chem. Int. Ed. Engl.* **1996**, *35*, 1838–1840. [CrossRef]
117. Danon, J.J.; Krüger, A.; Leigh, D.A.; Lemonnier, J.F.; Stephens, A.J.; Vitorica-Yrezabal, I.J.; Woltering, S.L. Braiding a molecular knot with eight crossings. *Science* **2017**, *355*, 159–162. [CrossRef]
118. Zhang, L.; Stephens, A.J.; Lemonnier, J.F.; Pirvu, L.; Vitorica-Yrezabal, I.J.; Robinson, C.J.; Leigh, D.A. Coordination chemistry of a molecular pentafoil knot. *J. Am. Chem. Soc.* **2019**, *141*, 3952–3958. [CrossRef]
119. Sohncke, L. *Entwickelung Einer Theorie der Krystallstruktur*; B.G. Teubner: Leipzig, Germany, 1879.